American Mineralogist, Volume 83, pages 1037–1044, 1998

The effect of trace elements on the olivine-wadsleyite transformation

Gudmundur H. Gudfinnsson and Bernard J. Wood*

Center for Experimental and Theoretical Study of the Earth's Interior, Department of Geology, University of Bristol, Bristol BS8 1RJ, U.K.

Abstract

Multianvil experiments were conducted at 1400 to 1600 °C on olivine and peridotite starting compositions to determine the partitioning of Ti, Al, Cr, Ni, Ca, and Na between coexisting olivine and wadsleyite. All of these elements occur as minor amounts in mantle olivine. Our experiments indicate that all, except Ca, partition preferentially into wadsleyite relative to olivine. The order of preference for wadsleyite is Ni<Na<Cr<Ti<Al, with $D_{tr}^{wad/ol}$ of about 2 for Ni, 3 for Na, and between 5 and 8 for Cr, Ti, and Al. We observe a strong negative correlation between the Si and Cr (+Al) contents of wadsleyite, indicating a coupled substitution of $2Cr^{3+}$ for $Mg^{2+} + Si^{4+}$. Modeling the influence of the trace elements on the olivine-wadsleyite transformation in the mantle indicates broadening effects on the order of 1–3 km, much smaller than that predicted to arise from mantle concentrations of H_2O. Therefore, effects of these trace elements on the properties of the 410 km seismic discontinuity are considered negligible. The maximum solubility of TiO_2 in wadsleyite (about 0.6%) is consistent with the suggestion that olivines containing about 1 vol% $FeTiO_3$ could be inverted wadsleyite.

Introduction

The 410 km seismic discontinuity, which marks the beginning of the mantle transition zone, is generally attributed to the transformation of olivine, the upper mantle's most abundant mineral, to wadsleyite [β-$(Mg,Fe)_2SiO_4$]. Seismological observations indicate that the discontinuity is narrow, frequently less than 10 km wide, and locally as narrow as 4 km (Benz and Vidale 1993; Yamazaki and Hirahara 1994). In contrast, phase diagrams for the Mg_2SiO_4-Fe_2SiO_4 system tend to suggest a broader transition interval and that olivine of mantle composition with Mg/(Mg+Fe) = 0.9 would transform to wadsleyite through a binary loop of 10–20 km width (Katsura and Ito 1989; Akaogi et al. 1989). The width of the two-phase loop is important because it is sensitive to both temperature (Bina and Helffrich 1994) and composition (Wood 1995) and therefore provides the potential for seismological data to constrain the thermal state and composition of the mantle. However, several sources of error exist that need to be addressed. One of these is the effect of garnet and pyroxene in mantle peridotite. These two phases tend to narrow the olivine-wadsleyite loop by buffering the Mg/Fe ratios of the coexisting $(Mg,Fe)_2SiO_4$ minerals (Stixrude 1997). The phase diagram for the Mg_2SiO_4-Fe_2SiO_4 system is itself subject to uncertainty in pressure and composition and Helffrich and Wood (1996) have shown that, taking account of these the uncertainties, the Mg_2SiO_4-Fe_2SiO_4-loop could be as narrow as 4 km for mantle olivine at a reasonable temperature for the 410 km seismic discontinuity of 1773 K. Finally, the chemical complexity of the mantle, relative to experimentally studied compositions may, as discussed below, broaden the transformation interval.

To date, virtually all comparisons of the olivine-wadsleyite transition interval with seismological data have used the simple Mg_2SiO_4-Fe_2SiO_4 system as a model. In the mantle, however, significant concentrations of minor elements, such as Ni, Cr, Al, and H, exist that could alter the stabilities of the two phases relative to the simple system and hence affect the depth and thickness of the 410 km discontinuity (Wood 1995; Wood et al. 1996). Wood (1995) argued that a trace element that is preferentially incorporated into wadsleyite would tend to stabilize this phase to lower pressure and would broaden the olivine-wadsleyite transformation interval. Conversely, if a trace element prefers olivine to wadsleyite, it would tend to expand the stability field of olivine to higher pressure. Water is one component that could have a particularly dramatic effect on the phase transformation. Water dissolves readily into wadsleyite by protonation of the O(1) atom and production of an Mg vacancy, as well as by population of the bridging O and other sites (Smyth 1987; Downs 1989; Young et al. 1983). Furthermore, measured partitioning between wadsleyite and olivine indicates that H_2O prefers the former by a ratio of about 20:1 (Kohlstedt et al. 1996). Assuming disorder of the point defects, as little as 500 ppm by weight of H_2O in the mantle could widen the olivine-wadsleyite transition interval by 15 km (Wood 1995). Other minor components, which are even more abundant than H_2O in the

* E-mail: b.j.wood@bris.ac.uk

0003–004X/98/0910–1037$05.00

TABLE 1. Starting compositions

Mixture	Composition
Fo90	$(Mg_{0.9}Fe_{0.1})_2SiO_4$
90NC	$(Mg_{0.9}Fe_{0.1})_2SiO_4$ + 1% NiO + 1% Cr_2O_3
90AT	$(Mg_{0.9}Fe_{0.1})_2SiO_4$ + 1% Al_2O_3 + 1% TiO_2
85NC	$(Mg_{0.85}Fe_{0.15})_2SiO_4$ + 1% NiO + 1% Cr_2O_3
85AT	$(Mg_{0.85}Fe_{0.15})_2SiO_4$ + 1% Al_2O_3 + 1% TiO_2
MPY-90	46.5% SiO_2, 0.22% TiO_2, 4.82% Al_2O_3, 6.24% FeO, 37.8% MgO, 3.54% CaO, 0.42% Na_2O, 0.45% Cr_2O_3

Note: All percentages are by weight.

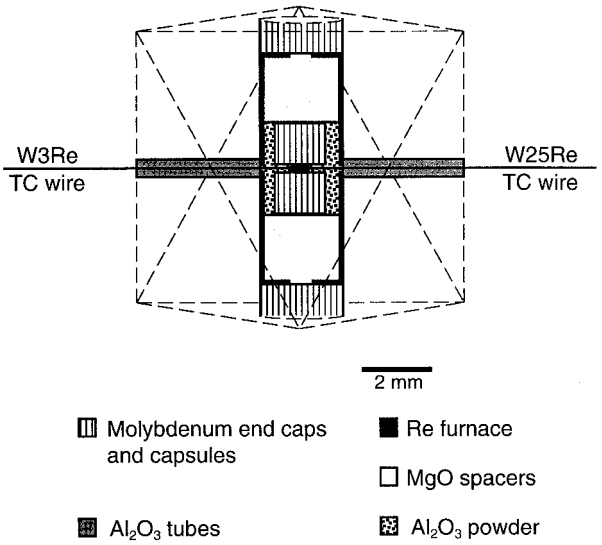

FIGURE 1. Cross section through the sample assembly. Dashed lines indicate outlines of Ceramacast octahedron.

upper mantle, could, in principle, have equally important effects on the transition. They could also provide clues as to the deep origins of some mantle rocks. Dobrzhinetskaya et al. (1996) have, for example, found very high concentrations of $FeTiO_3$ and chromite as precipitates in olivine from the Alpe Arami peridotite massif in Switzerland and proposed that these olivines originally crystallized as wadsleyite in the mantle transition zone. Experimental data on the relative solubilities of Ti and Cr in olivine and wadsleyite could clearly help test this hypothesis.

Because of their potential effects on mantle properties, we have performed high-pressure, high-temperature experiments on the solubilities of the most important minor elements in olivine and wadsleyite and measured their partitioning between the two phases. The data have been used to calculate the effects of these elements on the olivine-wadsleyite loop and hence on the 410 km seismic discontinuity. Modeling the width of the loop is necessary because at mantle concentration levels, less than several weight percent of an element, its effect on the transition interval is too small to be reproduced reliably in the multi-anvil apparatus.

EXPERIMENTAL METHODS

Five of the six different starting mixtures are sintered olivine compositions containing either 0 or 1 wt% NiO, Cr_2O_3, Al_2O_3, or TiO_2 (Table 1). They were prepared by mixing analytical grade oxide powders, pressing into pellets and then heating at 1400 °C for 1 h at an f_{H_2O} of FMQ-2 log units. Quenching was followed by grinding in an agate mortar, repressing and resintering. A total of three heatings and three grindings was used. X-ray diffraction of the reacted mixtures showed that they are all well-crystallized olivine. Only Ti-containing compositions contain small amounts of a second phase, ilmenite. The sixth composition (Table 1) is an MPY-90 peridotite (Falloon and Green 1987). This was prepared from a mixture of oxides and carbonates, which was decarbonated and then reduced at 950 °C and an f_{H_2O} of FMQ-2 log units for 24 h. X-ray diffraction indicated a poorly crystalline mixture of olivine and unreacted oxides.

Experiments were performed using a multianvil apparatus of the Walker et al. (1990) design. The tungsten carbide anvils had 5 mm truncations, gaskets were made of pyrophyllite and the pressure medium was a Ceramacast (Aremco Inc.) octahedron with 10 mm edge (Fig. 1). Pressure was calibrated by reproducing the I-II, II-III, and III-V transitions of Bi at room temperature, by bracketing the coesite-stishovite transition at 1000 °C and the forsterite-wadsleyite transition at 1200 °C, and from the compositions of coexisting olivine and wadsleyite and wadsleyite and ringwoodite in Fo_{90} bulk composition at 1200–1600 °C. Several of our experiments contained pure Fo_{90} as one of six simultaneously pressurized starting mixtures (see below). The compositions of coexisting olivine and wadsleyite in these experiments provide us with internal pressure calibrants. From the pressure reproducibility in these Fo_{90} experiments, the maximum uncertainty in pressure is estimated as 5% (±0.75 GPa at 15 GPa). Temperature was controlled to ±10 °C using a W3Re/W25Re thermocouple (Fig. 1).

Thermocouple emf was not corrected for the effect of pressure. In the first few experiments (NC or AT appended to the experiment number in Table 2). The sample was simply packed around the thermocouple, confined by the Re furnace and MgO spacers, without the use of a capsule. Microprobe analyses indicated negligible interaction of the sample with the furnace and the thermocouple, with a narrow region of reaction between the sample and the MgO spacers. To improve efficiency, later experiments used two molybdenum capsules, one on each side of the thermocouple junction. Each capsule had three sample holes that allowed us to perform experiments with up to six different starting compositions simultaneously.

The experiments were conducted at pressures from 13.0 to 14.2 GPa, at temperatures from 1200 to 1600 °C, with typical durations of 0.5 to 4 h. Experiments conducted at 1200 °C were incompletely reacted, even after several hours. At temperatures of 1400 °C and above, crystal sizes were on the order of 10 μm and hence could

generally be analyzed by electron microprobe. Although reversal experiments were not performed, we were able to judge, on textural and compositional grounds, which products most closely approached equilibrium. Texturally well-reacted samples were analyzed by microprobe and olivine-wadsleyite Fe-Mg partitioning used as an internal and external check (with data of Katsura and Ito 1989) on approach to equilibrium. Those experiment products that fulfilled these criteria and contain analyzable amounts of coexisting olivine and wadsleyite are listed in Table 2. From experiment textures and lack of homogeneity, we deduce that the experiments with the MPY-90 starting mixture take the longest to attain equilibrium and are most likely to be out of equilibrium. Because of the large temperature gradients in the octahedra (on the order of a few tens of degrees per millimeter), and correspondingly large variation in the proportion of the phases and their trace element contents, we analyzed and determined the trace element partitioning between pairs of adjacent crystals of olivine and wadsleyite. In addition to olivine and wadsleyite, the experimental products usually included other phases in lesser amounts. When the starting composition was olivine with Ni and Cr added, the products always contained small amounts of a Cr-rich phase with the same cation/oxygen ratio as garnet or pyroxene, whereas starting compositions of olivine with added Al and Ti had garnet and ilmenite as assessory phases, commonly as a fine intergrowth. In experiments with the peridotite composition of MPY-90, the main phase, in addition to olivine and wadsleyite, is garnet, but there are also small amounts of fine-grained anhydrous B, orthopyroxene, a silicate rich in Cr_2O_3 and CaO, perhaps clinopyroxene, and occasional unreacted magnesiowüstite, probably formed because of heterogeneities in the starting mixture.

Experimental products were analyzed using the JEOL 8600 microprobe in the Department of Geology at the University of Bristol. The analyses were conducted using a 15 kV accelerating potential and 15 nA beam current with approximately 1 μm probe diameter. Counting times were 20 s for the major elements, Si, Mg, and Fe, and 40 s for the trace elements, Ni, Cr, Al, Ti, Na, and Ca. Natural and synthetic minerals were used as standards, and the ZAF correction procedure was applied. It should be noted that it is almost impossible to completely eliminate water from starting mixtures in multianvil experiments. Indeed, small amounts of water persistently present in ''anhydrous'' experiments could explain the relatively broad olivine-wadsleyite loop measured experimentally (Wood 1995). To minimize the H_2O contents of our products, we fired the octahedra at 1000 °C before use and stored all of our sintered starting materials at 110 °C until just before loading into the capsule. The microprobe analyses provide some constraint on the H_2O contents of the products. Water prefers wadsleyite to olivine, and can in this phase approach the 3.3% of the fully hydrated endmember (Kohlstedt et al. 1996). Despite this, we did not find that wadsleyite had consistently lower electron-microprobe totals than olivine in our experimental products, and totals were generally between the 99 and 101 wt% expected for anhydrous minerals. We therefore believe that our synthetic olivines and wadsleyites contain only small amounts of water.

Partitioning and solubility of trace elements in olivine and wadsleyite

We have determined the partitioning of the most abundant of the elements in the mantle, Fe, Mg, Ni, Cr, Al, Ti, Ca, and Na between coexisting olivine and wadsleyite. Apart from H (Wood 1995; Wood et al. 1996), these are the only elements present in sufficient abundance to affect the width and depth of the olivine-wadsleyite transition. Figure 2 shows that Mg-Fe partitioning is in extremely good agreement with previous measurements of Katsura and Ito (1989), confirming that recrystallization has generated cation exchange and re-equilibration. In terms of the minor components, Ca is the only element that is preferably incorporated into olivine relative to wadsleyite in the ratio 2:1 (Table 2). The other elements become progressively more compatible in wadsleyite relative to olivine in the order Ni<Na<Cr<Ti<Al. Weight partition coefficients ($D_{tr}^{wad\text{-}ol}$ = wt% tr in wad/wt% tr in ol), increase from about two for Ni to approximately eight for Al (Table 2). The implications of these results for the olivine-wadsleyite transition interval will be discussed in a later section.

The maximum concentration of a minor element that can be accommodated in olivine and wadsleyite should be observed in experiments that are saturated in the element, i.e., contain a stable phase that is rich in the ''minor'' element. For example, in those experiments that used starting compositions of olivine plus 1% TiO_2, ilmenite was always found as an accessory phase. At ilmenite saturation the maximum TiO_2 content of wadsleyite was about 0.6% (Fig. 3), which we take to be the approximate level of saturation in Fe-bearing systems. The saturation level for olivine is only 0.1% TiO_2 (Fig. 3). Starting materials of olivine with 1% Cr_2O_3 produced Cr-rich accessory phases, wadsleyite containing up to 2% Cr_2O_3 and olivine with up to 0.35% Cr_2O_3. With 1% Al added to the olivine, small amounts of aluminous garnet were produced and the coexisting wadsleyite and olivine contained up to 0.4% and <0.1% Al_2O_3, respectively. Saturation with Ni was not seen. The fact that Cr, Ti, and Al have very low solubility in olivine exercises a considerable influence on wadsleyite-olivine partition coefficients and causes the scatter shown in the partitioning coefficients (Table 2). The reason can be understood by considering Cr as an example. In Figure 4 we have plotted D_{Cr} as a function of Mg/(Mg+Fe) of wadsleyite for all our experiments on Fo_{85} and Fo_{90} bulk compositions containing 1% Cr_2O_3. Each point on Figure 4 represents a single wadsleyite-olivine pair. Good correlations between X_{Mg} and D_{Cr} can be seen in both cases. For any given olivine bulk composition, the first wadsleyite to appear has the lowest X_{Mg} and a Cr content close to satu-

TABLE 2. Experimental conditions, phase compositions, partition coefficients, and trace element concentrations

Experiment no.	Starting composition	Pressure (GPa)	Temperature (°C)	Duration (h)	Forsterite content*		Kd†	D_{Ti}‡	D_{Al}	D_{Cr}	D_{Ni}	D_{Ca}
					Olivine	Wadsleyite						
85MU1	85NC	13.2	1400	1.5	89.1(2)‖	82.8(1)	0.59(1)			5.2(4)	1.6(1)	
85MU1	85AT	13.2	1400	1.5	89.5(2)	80.3(2)	0.48(1)	6.1(6)	21(2)			
90NC6	90NC	13.7	1400	1	92.5(2)	88.2(2)	0.60(2)			5.9(7)	1.8(1)	
85NC2	85NC	13.7	1600	1	87.7(4)	78.2(5)	0.50(2)			11(2)	1.9(1)	
85AT4	85AT	13.8	1600	1	88.5(2)	79.1(3)	0.49(1)	11(2)	17(3)			
85AT3	85AT	13.8	1600	1	89.3(2)	78.5(4)	0.44(1)	7.9(20)	14(3)			
90AT8	90AT	14.1	1600	1	91.9(3)	82.8(4)	0.42(2)	7.1(15)	11(2)			
90NC5	90NC	14.1	1600	1	91.7(2)	85.0(3)	0.51(2)			9.4(7)	2.4(2)	
90MU3	Fo90	14.1	1600	0.75	91.2(1)	84.6(4)	0.54(2)					
90MU3	90NC	14.1	1600	0.75	92.9(1)	88.3(2)	0.58(1)			5.0(4)	2.1(1)	
90MU3	90AT	14.1	1600	0.75	92.1(1)	85.3(3)	0.50(1)	4.9(5)	6.7(8)			
90MU3	MPY-90	14.1	1600	0.75	89.1(2)	80.2(3)	0.49(1)	12(2)	5.4(7)	4.1(5)		0.41(12)
90MU5	Fo90	14.2	1600	1	92.9(2)	88.6(2)	0.59(2)					
90MU5	90NC	14.2	1600	1	93.2(1)	89.1(1)	0.59(1)			4.9(2)	2.2(1)	
90MU5	90AT	14.2	1600	1	92.9(2)	88.2(2)	0.57(2)	7.9(12)	12(1)			
90MU5	MPY-90	14.2	1600	1	92.9(2)	88.2(2)	0.57(2)	8.5(14)	6.3(8)	3.4(3)		0.97(35)
Weighted mean								6.3	7.7	4.9	1.9	0.47

* Molar Mg/(MG + FE)·100.
† $Kd = (X^{ol}_{Fe} \cdot X^{wad}_{Mg})/X^{ol}_{Mg} \cdot X^{wad}_{Fe})$.
‡ $D_{tr} = D^{wad-ol}_{tr}$.
§ Concentrations of oxides in weight percent.
‖ Values within () denote standard errors on the last digit. In the case of oxide concentrations standard errors are derived from 6–12 individual electron microprobe analyses and in the case of forsterite content and partition coefficients they are propagated standard errors.

ration (about 2% Cr_2O_3). As the amount of wadsleyite increases, so does its X_{Mg} whereas its Cr content must decrease toward the 1% Cr_2O_3 of the bulk composition. The wadsleyite-olivine partition coefficient would remain constant if Cr substitution followed Henry's Law region in both phases. However, because the saturation value for olivine is only around 0.3% Cr_2O_3, this phase is essentially always saturated and in the region where small changes in Cr content correspond to large changes in activity, i.e., highly non-ideal. Thus, whereas wadsleyite approaches Henry's Law behavior for Cr substitution, olivine is highly non-ideal and D_{Cr} is a strong function of the Cr content and hence X_{Mg} of the wadsleyite.

The peridotite starting composition produced a pyropic garnet containing about 6% CaO and most of the Ti and Cr in the bulk composition. The Cr and Ti-rich phases discussed above did not appear so, as expected, the Cr and Ti contents of olivine and wadsleyite are substantially below saturation at up to 0.9% and 0.2% in wadsleyite, respectively. Despite the lower concentrations, partitioning relationships of Cr, Ti, and Al between the two $(Mg,Fe)_2SiO_4$ phases are essentially the same as those observed with olivine starting materials (Table 2). Variable Ca contents of about 0.1% were found in both phases. Possibly the variation is partially due to secondary fluorescence from adjacent Ca-rich phases such as garnet (Dalton and Lane 1996). The Ca results are not reliable. Wadsleyite was found to contain consistently more Na than adjacent olivine, with a maximum content of 0.2%.

Solution mechanism of Cr and Al in wadsleyite

From the crystal structures and compositions of synthetic wadsleyite (Inoue 1994), it is apparent that H enters the structure coupled to the formation of Mg vacancies (Smyth 1987). If we assume that H attaches to the O(1) atom as proposed by Smyth (1987), then the theoretical end-member $Mg_7Si_4O_{14}(OH)_2$, a composition close to which has been synthesized by Inoue (1994), has 12.5% of its Mg positions vacant. As shown above, the 3+ cation Cr^{3+} is quite soluble in wadsleyite (up to 2 wt%), and it is of interest to determine whether or not this also substitutes with the creation of cation vacancies. In Figure 5, we show all of our Cr-bearing wadsleyite analyses (from all experiments) plotted as Si to four O atoms vs. Cr to four O atoms. In this plot, analyses with cation totals to four O atoms of between 2.95 and 3.05 were used. The data fall very close to a straight line of slope −0.5 passing through the point where Cr is 0.0 and Si 2.0 (i.e., perfect olivine stoichiometry). The correlation is similarly good when Cr+Al are plotted against Si (Fig. 5).

Although the substitution mechanism of Cr^{3+} (or Al^{3+}) cannot always be determined unequivocally from stoichiometry alone, Figure 5 does, in this case, provide constraints on how dissolution takes place. This statement can be elaborated by considering the most likely solution mechanisms for Cr^{3+} (Al^{3+}) in wadsleyite. These are: (1) substitution of 2 Cr^{3+} for 3 Mg^{2+} with creation of a magnesium vacancy:

$$3Mg^{2+} = 2Cr^{3+} + \square^{11}_{Mg}. \quad (1)$$

Clearly, if Cr^{3+} dissolves in this manner, the Si content should remain constant at 2.0 per four O atoms and there should be no correlation between Cr and Si contents. (2) Replacement of 3 Si^{4+} by 4 Cr^{3+}, one of the latter being interstitial. The predicted slope of the Cr-Si plot is −0.75. (3) Replacement of 2 Si^{4+} by 2 Cr^{3+} with creation of an oxygen vacancy. The slope in this case would be −1.0. (4) Replacement of Mg^{2+} and Si^{4+} by 2 Cr^{3+}:

TABLE 2—*Continued.*

	Wadsleyite						Olivine					
D_{Na}	TiO_2§	Al_2O_3	Cr_2O_3	NiO	CaO	Na_2O	TiO_2	Al_2O_3	Cr_2O_3	NiO	CaO	Na_2O
		0.23(1)	0.91(3)	1.22(2)				0.02(0)	0.19(1)	0.77(3)		
	0.38(3)	0.35(2)					0.07(1)	0.03(0)				
		0.26(2)	1.37(8)	1.51(4)				0.04(0)	0.25(3)	0.81(4)		
		0.21(2)	2.01(21)	1.69(7)				0.02(0)	0.20(3)	0.96(5)		
	0.42(1)	0.29(3)					0.04(1)	0.02(0)				
	0.30(2)	0.23(20)					0.03(1)	0.02(0)				
	0.24(2)	0.22(3)					0.04(1)	0.02(0)				
		0.22(2)	2.19(12)	2.05(12)				0.01(0)	0.24(1)	0.87(6)		
		0.29(2)	1.70(11)	1.53(7)				0.03(0)	0.35(2)	0.74(3)		
	0.49(3)	0.34(2)					0.11(1)	0.05(1)				
3.0(4)	0.13(1)	0.42(3)	0.94(8)		0.06(1)	0.24(2)	0.02(1)	0.08(1)	0.23(2)		0.21(9)	0.08(1)
		0.25(1)	1.27(3)	1.21(6)				0.02(1)	0.26(1)	0.57(3)		
	0.63(6)	0.26(1)					0.09(1)	0.02(0)				
2.8(2)	0.17(2)	0.43(3)	0.69(5)		0.11(4)	0.21(1)	0.02(0)	0.08(1)	0.20(1)		0.11(1)	0.08(1)
2.8												

$$Mg^{2+} + Si^{4+} = Cr^{3+} + Cr^{3+}. \quad (2)$$

In this case the predicted slope is in agreement with that observed, −0.5. Stoichiometrically, then, this is the correct replacement mechanism. At first sight it implies that Cr^{3+} is entering both tetrahedral sites and octahedral sites, replacing Si on the former and Mg on the latter. A more reasonable interpretation, however, given the strong octahedral preference of Cr^{3+}, is that Mg^{2+} replaces tetrahedral Si^{4+} leaving Cr^{3+} exclusively in octahedral sites:

$$2^{[6]}Mg^{2+} + {}^{[4]}Si^{4+} = {}^{[4]}Mg^{2+} + 2^{[6]}Cr^{3+}. \quad (3)$$

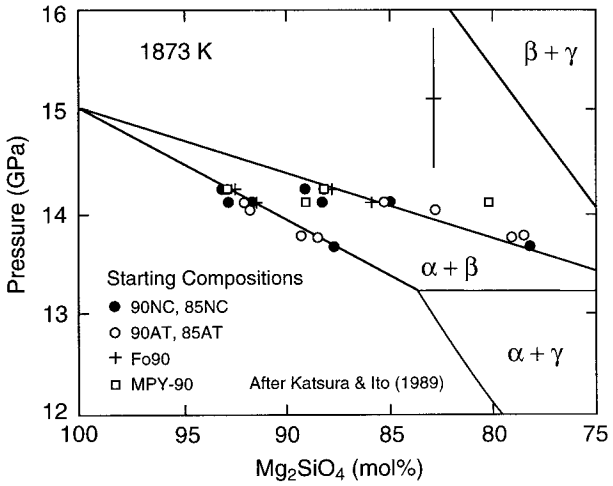

FIGURE 2. Pressure-composition diagram for the system Mg_2SiO_4-Fe_2SiO_4 from Katsura and Ito (1989) showing the olivine-wadsleyite loop at 1773 K. The symbols indicate compositions of coexisting olivine and wadsleyite in our experiments. The pressures of the experiments have been adjusted so that the points fall close to the two-phase loop. The cross denotes approximate propagated standard errors in the compositions and 5% uncertainty in pressure. All pressure adjustments are within this uncertainty.

This substitution would be analogous to that observed in spinels with the addition of the $MgCr_2O_4$ component.

THE EFFECT OF TRACE ELEMENTS ON THE 410 KM DISCONTINUITY

The effect of a trace element on the stability of coexisting wadsleyite and olivine in pressure-composition space can be evaluated by considering its effects on the partial molar free energies of the Mg_2SiO_4 and Fe_2SiO_4 components in the two Mg_2SiO_4-Fe_2SiO_4 solid-solutions. For coexisting olivine and wadsleyite we can consider the equilibria:

$$Mg_2SiO_4\ (\text{olivine}) = Mg_2SiO_4\ (\text{wadsleyite}) \quad (4)$$

$$Fe_2SiO_4\ (\text{olivine}) = Fe_2SiO_4\ (\text{wadsleyite}). \quad (5)$$

Concentrating for the moment on the Mg_2SiO_4 component, we express the equilibrium conditions as follows:

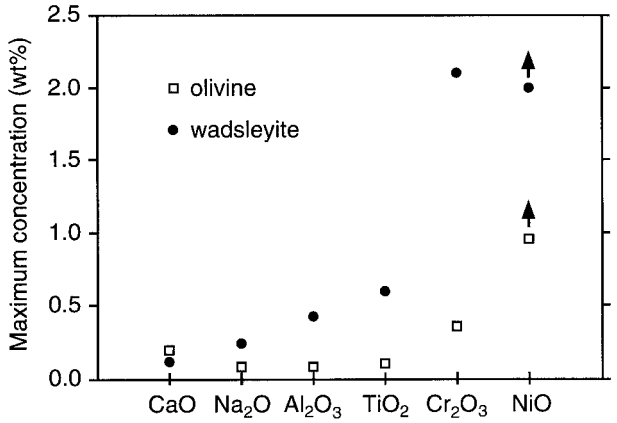

FIGURE 3. Maximum solubility of trace elements observed in the experiments. Arrows indicate that solubility is limited only by the amount of trace element present.

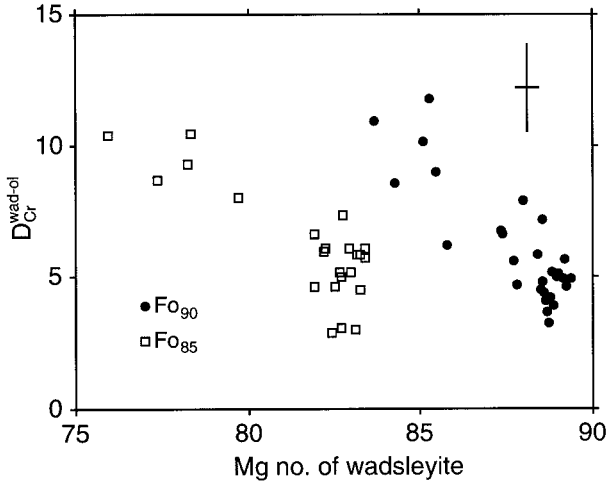

FIGURE 4. Partitioning of Cr between pairs of adjacent wadsleyite and olivine crystals as a function of 100 × Mg/(Mg+Fe) of wadsleyite crystal. The open symbols indicate partitioning in experiments where the bulk composition was Fo_{90} and the solid symbols Fo_{85}. Error bars indicate approximate propagated standard errors.

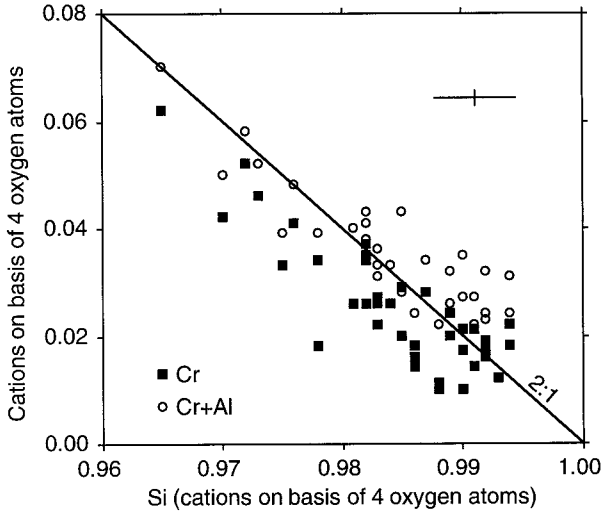

FIGURE 5. Correlation between Cr or Cr+Al and Si in all individual analyses of wadsleyite. Notice that the diagonal line does not indicate a regression fit. Error bars denote standard deviation.

$$\mu^{wad}_{Mg_2SiO_4} = \mu^{ol}_{Mg_2SiO_4} \quad (6)$$

and

$$\mu^{ol}_{Mg_2SiO_4} = \mu^{0}_{Mg_2SiO_4} + RT \ln a^{ol}_{Mg_2SiO_4} \quad (7)$$

$$\mu^{wad}_{Mg_2SiO_4} = \mu^{0}_{Mg_2SiO_4} + RT \ln a^{wad}_{Mg_2SiO_4}. \quad (8)$$

If, for olivine and wadsleyite, we take the standard state chemical potential $\mu^0_{Mg2SiO4}$ to be equal to the molar free energy of the respective pure phase at the pressure and temperature of interest, then, by substituting Equations 7 and 8 into Equation 6 and taking into account the effect of pressure on the free energy of the reaction, we find a relationship between the equilibrium pressure, *P*, for coexisting olivine-wadsleyite solid solutions, at temperature, *T*, and the activity of Mg_2SiO_4 component in the two phases as follows (Wood 1990):

$$\int_{P^0}^{P} \Delta V^0 \, dP = -RT \ln a^{wad}_{Mg_2SiO_4} + RT \ln a^{ol}_{Mg_2SiO_4} \quad (9)$$

where P^0 is the pressure of equilibrium of pure Mg_2SiO_4 wadsleyite and olivine at temperature *T*. To a very good approximation *P* and P^0 are so close together that ΔV^0, the volume change of the reaction of pure Mg_2SiO_4 can be treated as a constant to give:

$$\Delta V^0(P - P^0) \cong -RT \ln a^{wad}_{Mg_2SiO_4} + RT \ln a^{ol}_{Mg_2SiO_4}. \quad (10)$$

At 14.5 GPa and 1773 K, the approximate conditions of the 410 km discontinuity, ΔV^0 is calculated to be −2.24 cm^3 (Wood et al. 1996). In order to obtain *P* and hence the effect of the substituent ions on the transition pressure, we now need to estimate the relationships between activity and composition of the two phases. If we make the simplest assumption, that the octahedral Mg, Fe, and trace cations are completely disordered over the crystallographically different sites in the structure, then activity $a^{ol}_{Mg_2SiO_4}$ and $a^{wad}_{Mg_2SiO_4}$ are related to composition as follows:

$$a^{wad}_{Mg_2SiO_4} = (X_{Mg}\gamma_{Mg})^2(X_{Si}\gamma_{Si}) \quad (11)$$

where X_{Mg} and γ_{Mg} refer to the atomic fraction of Mg atoms on the octahedral sites and the activity coefficient for Mg on these sites, respectively. Tetrahedral site occupancy of Si and its activity coefficient are represented by X_{Si} and γ_{Si}. Activity-composition relations for Mg_2SiO_4-Fe_2SiO_4 olivine solutions have been measured by solution calorimetry (Wood and Kleppa 1981; Kojitani and Akaogi 1994) and experimentally by phase equilibria (e.g., Wiser and Wood 1991; von Seckendorff and O'Neill 1993). For Mg-Fe mixing there is a small positive deviation from ideality ($\gamma_{Mg} > 1$) and the activity coefficient obeys the symmetrical solution model (see, for example, Thompson 1967). In our study there were two trace elements in each experiment in addition to Mg and Fe, so we need to extend the symmetrical solution equations to four components as follows (after Helffrich and Wood 1989):

$$\begin{aligned} RT \ln \gamma_{Mg} = {} & W_{FeMg}X_{Fe}(1 - X_{Mg}) + W_{iMg}X_i(1 - X_{Mg}) \\ & + W_{jMg}X_j(1 - X_{Mg}) - W_{ij}X_iX_j \\ & - W_{jFe}X_jX_{Fe} - W_{iFe}X_iX_{Fe}. \end{aligned} \quad (12)$$

In Equation 12, subscripts i and j refer to the two trace elements i and j and W_{iMg} refers to the symmetrical interaction parameter between i atoms and Mg atoms on the octahedral sites. Extension to more components follows simply in the same form as Equation 12. Because i and j are present in low concentration, $X_i \approx X_j \approx 0$ and Equation 12 simplifies to:

TABLE 3. The effect of trace elements on the 410 km discontinuity

Element	Max wt% in olivine	Max wt% in wadsleyite	$D_{tr}^{wad/ol}$	Broadening* (km)	Depth† (km)
NiO	0.5	0.95	1.9	0.9	−1.8
Cr_2O_3	0.18	0.73	4.0	2.7	−3.6
Al_2O_3	0.05	0.35	6.0	2.8	−3.3
TiO_2	0.03	0.2	6.3	0.5	−0.6
Na_2O	0.07	0.2	2.8	0.8	−1.3

Notes: Calculations performed at 1773 K. In the absence of trace elements, the transition interval is calculated to be 7.5 km. Substitution assumed to be in octahedral sites unless noted otherwise in text.

* Broadening of the transformation interval caused by incorporation of the trace element into Fo_{90} olivine.

† Height of the discontinuity relative to the trace-element free system. Negative numbers indicate elevation.

$$RT\ln\gamma_{Mg} \cong W_{FeMg}X_{Fe}(1 - X_{Mg}). \quad (13)$$

Experimental measurements at 1200 K (Wiser and Wood 1991) indicate that for olivine, W_{FMg}^{ol} is 3.7 ± 0.8 kJ/mol of Fe-Mg atoms. With excess volumes of mixing this becomes approximately 5.0 kJ at the pressure of the transition (Wood et al. 1996). Fitting of the olivine-wadsleyite loop in the Mg_2SiO_4-Fe_2SiO_4 system by Akaogi et al. (1989) and by Fei et al. (1991) indicates that $W_{FeMg}^{wad} < W_{FeMg}^{ol}$ by about 1 kJ. This provides sufficient constraint, as will be shown below, for accurate modeling of the effects of different minor components in the two phases. Because the Si site is more than 96% occupied by Si atoms, even in the most dilute cases shown in Figure 5, it is reasonable to assume Raoults Law behavior for the major component, yielding $\gamma_{Si} \cong 1.0$.

The final piece of information required to apply Equation 13 is the distribution of the trace elements between the octahedral and tetrahedral sites in olivine and wadsleyite structures. For Ni we assumed random mixing on the octahedral (Mg, Fe) sites only, whereas for Cr and Al we assumed coupled substitution according to Equation 3 with the trivalent ions entering octahedral positions and Mg replacing Si in tetrahedral coordination. Because we were unable to clarify the charge-balancing mechanism for Ti and Na, we assumed random mixing on octahedral sites only.

Approximate concentrations in the two phases were derived from the partitioning experiments on the peridotite bulk composition after constraining partition coefficients to be consistent with the broader experimental data set. For Cr, Al, Ti, and Na the maximum concentrations in olivine are broadly consistent with those found in olivines from lherzolite xenoliths (Hervig et al. 1986). For NiO we assumed a maximum of 0.5% in olivine, a value also consistent with measurements on mantle xenoliths (Hervig et al. 1986). The concentrations in the two phases were assumed to vary through the transition loop in accordance with the lever rule. Alternative compositional models are discussed below.

At 1773 K, our model without trace elements gave a width of the transition interval as 7.5 km. None of the minor elements, at the concentration levels present in the mantle, is predicted to broaden the transition interval by more than 2.8 km (Table 3). Changes in the overall depth of the transition at 1773 K are also extremely small, at 3.6 km or less. The results confirm that H is the only element able to effect large changes in the transition interval at plausible mantle concentration levels. Wood (1995), for example, calculated that the transition interval could broaden by 15 km if there were 500 ppm by weight of H_2O in olivine at 410 km depth.

DISCUSSION

The calculations described above involve a number of assumptions many of which can be debated. To determine whether or not the conclusions are robust we repeated many of the calculations of Table 3 making alternative assumptions as follows: (1) Uncertainty in the Fe-Mg mixing properties of olivine. The calculations assumed W_{FeMg}^{ol} of 5.0 kJ and W_{FeMg}^{wad} of 4.0 kJ. We repeated most of them with W_{FeMg}^{ol} of 7.0 kJ and W_{FeMg}^{wad} of 3.0 kJ, values that almost certainly overestimate the differences between olivine and wadsleyite (Akaogi et al. 1989; Fei et al. 1991). The effect on all results in Table 3 is on the order of 0.01 km. (2) Unbuffered as opposed to buffered trace element contents. We assumed that the trace element content of olivine at 410 km is transferred progressively to wadsleyite through the transition interval without the involvement of other phases, i.e., it is unbuffered. In some cases, however, notably Al, Cr, and Ti, there is in the mantle a phase rich in these elements, garnet, which will tend to fix or buffer the contents of olivine and wadsleyite at constant values. If fixed concentrations are assumed in olivine and wadsleyite, then the broadening of the transition is reduced to <0.01 km, but the change in the depth of the discontinuity is unaffected. (3) Ti replacing Si on tetrahedral sites instead of Mg on octahedral sites. The effect is negligible. (4) Cation ordering in wadsleyite. Sawamoto and Horiuchi (1990) synthesized a single crystal of wadsleyite of composition $(Mg_{0.9}Fe_{0.1})_2SiO_4$ at 2000 °C and 18–20 GPa, and found ordering of Mg and Fe on the octahedral sites such that the mole fraction of Mg on M1 site was 0.89, 0.95 on the M2 site, and 0.88 on the M3 site. We used these partitioning relationships and found that they could broaden the discontinuity slightly, or by about 0.5 km in the absence of trace elements. We then made the conservative assumption that Ni is completely ordered onto ¼ of the octahedral sites, equivalent to assuming complete ordering on M1 or on M2, and repeated the calculations. The broadening due to the trace element remains exactly the same as that shown in Table 3. (5) Uncertainty in the ΔV^0 of reaction. Uncertainties in thermal expansion and compressibility could cause a significant error in the volume change of the reaction. As an illustration, the parameters used here indicate that the transformation of olivine to wadsleyite begins if Mg/(Mg+Fe) has the mantle value of 0.90 and temperature is 1773 K at 0.75 GPa below the transformation in pure Mg_2SiO_4. The best-fit Mg_2SiO_4-Fe_2SiO_4 phase diagrams of

Akaogi et al. (1989) and Katsura and Ito (1989) suggest a slightly larger change of 1.0 GPa. If they were correct and the error were entirely due to volume uncertainties then the ΔV^0 of the reaction used by us would be about 25% too large. The values given in Table 3 would then need to be multiplied by 1.33. A very conservative estimate of the volume error would be that the values in Table 3 are too small by a factor of two. Even in this case the effects remain very small.

Our results demonstrate that the maximum concentrations of TiO_2 and Cr_2O_3 that can dissolve in wadsleyite are on the order of 0.6 and 2.0 wt%, respectively, at 14 GPa and 1873 K. Dobrzhinetskaya et al. (1996) report that olivines in the Alpe Arami Massif, Switzerland contain high Ti and Cr, about 1 vol% of exsolution lamellae of $FeTiO_3$ and about 0.25% chromite lamellae. If these exsolved from an initially homogeneous $(Mg,Fe)_2SiO_4$ solid solution, then the latter originally contained about 0.5% TiO_2 and 0.2% Cr_2O_3. Our results clearly show that wadsleyite can accommodate these concentrations of Ti and Cr in appropriate bulk compositions and that they are feasible, even in fertile peridotite. Our results appear to be consistent with the hypothesis that the relict porphyroclastic olivine in the Alpe Arami Massif originally formed as wadsleyite.

Acknowledgments

We thank Bruno Reynard and an anonymous reviewer for invaluable comments that led to significant improvements in this paper, and Andy Robinson for providing a sample of composition MPY-90. This research was supported by NERC grant GR3/10120.

References cited

Akaogi, M., Ito, E., and Navrotsky, A. (1989) Olivine-modified spinel-spinel transitions in the system Mg_2SiO_4-Fe_2SiO_4: Calorimetric measurements, thermochemical calculation, and geophysical application. Journal of Geophysical Research, 94, 15671–15685.

Benz, H. and Vidale, J. (1993) Sharpness of upper-mantle discontinuities determined from high-frequency reflections. Nature, 365, 147–150.

Bina, C.R. and Helffrich, G.R. (1994) Phase transition Clapeyron slopes and transition zone seismic discontinuity topography. Journal of Geophysical Research, 99, 15853–15860.

Dalton, J.A. and Lane, S.J. (1996) Electron-microprobe analysis of Ca in olivine close to grain boundaries: The problem of secondary X-ray fluorescence. American Mineralogist, 81, 194–201.

Dobrzhinetskaya, L., Green, H.W., and Wang, S. (1996) Alpe Arami: A peridotite massif from depths of more than 300 kilometers. Science, 271, 1841–1845.

Downs, J.W. (1989) Possible sites for protonation in β-Mg_2SiO_4 from an experimentally derived electrostatic potential. American Mineralogist, 74, 1124–1129.

Falloon, T.J. and Green, D.H. (1987) Anhydrous partial melting of MORB pyrolite and other peridotite compositions at 10 kb: Implications for the origin of primitive MORB glasses. Contributions to Mineralogy and Petrology, 37, 181–219.

Fei, Y., Mao, H.-K., and Mysen, B.O. (1991) Experimental determination of element partitioning and calculation of phase relations in the MgO-FeO-SiO_2 system at high pressure and high temperature. Journal of Geophysical Research, 96, 2157–2170.

Helffrich, G.R. and Wood, B.J. (1989) Subregular model for multicomponent solutions. American Mineralogist, 74, 1016–1022.

——(1996) 410 km discontinuity sharpness and the form of the olivine α-β phase diagram: Resolution of apparent seismic contradictions. Geophysical Journal International, 126, F7–F12.

Hervig, R.L., Smith, J.V., and Dawson, J.B. (1986) Lherzolite xenoliths in kimberlites and basalts: petrogenetic and crystallochemical significance of some minor and trace elements in olivine, pyroxenes, garnet and spinel. Transactions of the Royal Society of Edinburgh, Earth Sciences, 77, 181–201.

Inoue, T. (1994) Effect of water on melting phase relations and melt composition in the system Mg_2SiO_4-$MgSiO_3$-H_2O up to 15 GPa. Physics of the Earth and Planetary Interiors, 85, 237–263.

Katsura, T. and Ito, E. (1989) The system Mg_2SiO_4-Fe_2SiO_4 at high pressures and temperatures: Precise determination of stabilities of olivine, modified spinel, and spinel. Journal of Geophysical Research, 94, 15663–15670.

Kohlstedt, D.L., Keppler, H., and Rubie, D.C. (1996) Solubility of water in the α, β and γ phases of $(Mg,Fe)_2SiO_4$. Contributions to Mineralogy and Petrology, 123, 345–357.

Kojitani, H. and Akaogi, M. (1994) Calorimetric study of olivine solid solutions in the system Mg_2SiO_4-Fe_2SiO_4. Physics and Chemistry of Minerals, 20, 536–540.

Sawamoto, H. and Horiuchi, H. (1990) β $(Mg_{0.9}, Fe_{0.1})_2SiO_4$: Single crystal structure, cation distribution, and properties of coordination polyhedra. Physics and Chemistry of Minerals, 17, 293–300.

Smyth, J.R. (1987) β-Mg_2SiO_4: A potential host for water in the mantle? American Mineralogist, 72, 1051–1055.

Stixrude, L. (1997) Structure and sharpness of phase transitions and mantle discontinuities. Journal of Geophysical Research, 102, 14835–14852.

Thompson, J.B. (1967) Thermodynamic properties of simple solutions. In P.H. Abelson, Ed., Researches in Geochemistry, 2, 340–361, Wiley, New York.

von Seckendorff, V. and O'Neill, H.S.C. (1993) An experimental study of Fe-Mg partitioning between olivine and orthopyroxene at 1173, 1273 and 1423 K and 1.6 GPa. Contributions to Mineralogy and Petrology, 113, 196–207.

Walker, D., Carpenter, M.A., and Hitch, C.M. (1990) Some simplifications to multianvil devices for high pressure experiments. American Mineralogist, 75, 1020–1028.

Wiser, N.M. and Wood, B.J. (1991) Experimental determination of activities in Fe-Mg olivine at 1400 K. Contributions to Mineralogy and Petrology, 108, 146–156.

Wood, B.J. (1990) Postspinel transformations and the width of the 670-km discontinuity: A comment on ''Postspinel transformations in the system Mg_2SiO_4-Fe_2SiO_4 and some geophysical implications'' by E. Ito and E. Takahashi. Journal of Geophysical Research, 95, 12681–12685.

——(1995) The effect of H_2O on the 410-kilometer seismic discontinuity. Science, 268, 74–76.

Wood, B.J. and Kleppa, O.J. (1981) Thermochemistry of forsterite-fayalite olivine solutions. Geochimica et Cosmochimica Acta, 45, 529–534.

Wood, B.J., Pawley, A., and Frost, D.R. (1996) Water and carbon in the Earth's mantle. Philosophical Transactions of the Royal Society of London Series A, 354, 1495–1511.

Yamazaki, A. and Hirahara, K. (1994) The thickness of upper mantle discontinuities, as inferred from short-period J-Array data. Geophysical Research Letters, 21, 1811–1814.

Manuscript received October 22, 1997
Manuscript accepted March 30, 1998
Paper handled by Nancy Ross